

Electronic Supplementary Information

Photocurrents at polarized liquid|liquid interfaces enhanced by a gold nanoparticle film

Delphine Schaming,^a Mohamad Hojeij,^a Nathalie Younan,^a Hirohisa Nagatani,^{a,b} Hye Jin Lee^c and Hubert H. Girault*^a

^a Laboratoire d'Electrochimie Physique et Analytique, Ecole Polytechnique Fédérale de Lausanne, Station 6, CH-1015 Lausanne, Switzerland. Fax: +41 21 693 36 67; Tel: +41 21 693 31 45; E-mail: hubert.girault@epfl.ch

^b Faculty of Chemistry, Institute of Science and Engineering, Kanazawa University, Kakuma, Kanazawa 920-1192, Japan.

^c Department of Chemistry, Kyungpook National University, 1370 Sankyuk-dong, Buk-gu, Daegu-city, 702-701, Republic of Korea.

Characterization of the gold NPs

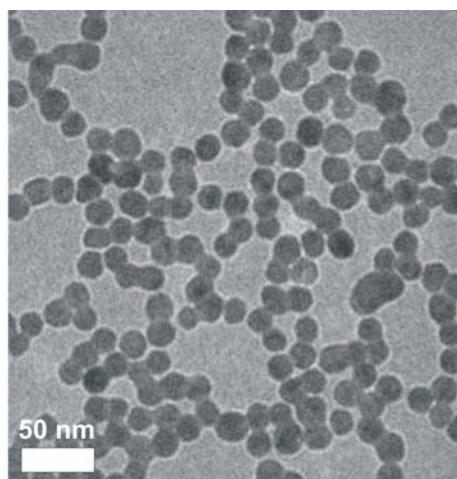


Fig. S1. TEM micrograph of the gold NPs.

UV-visible, photophysical and electrochemical studies of ZnTPPC

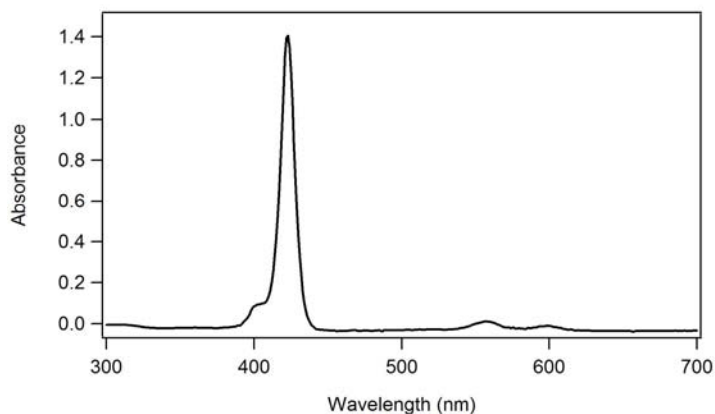


Fig. S2. UV-visible absorption spectrum of an aqueous solution of ZnTPPC (0.05 mM) (optical pathway: 0.1 cm).

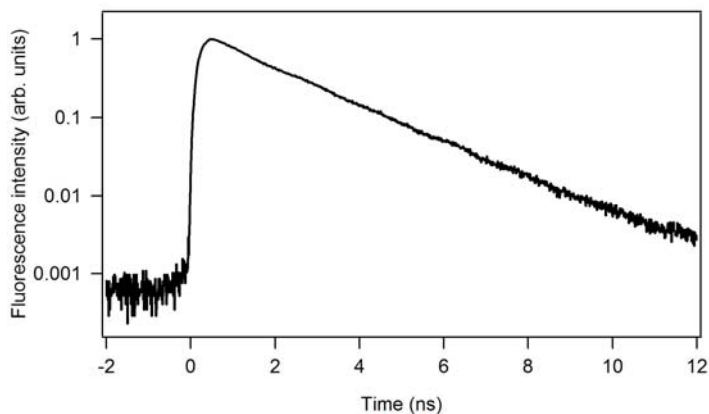


Fig. S3. Time resolved emission measurement for ZnTPPC (pH 5.8) at the water|DCE interface. $\lambda_{\text{exc}} = 440 \text{ nm}$ and $\lambda_{\text{em}} = 610 \text{ nm}$.

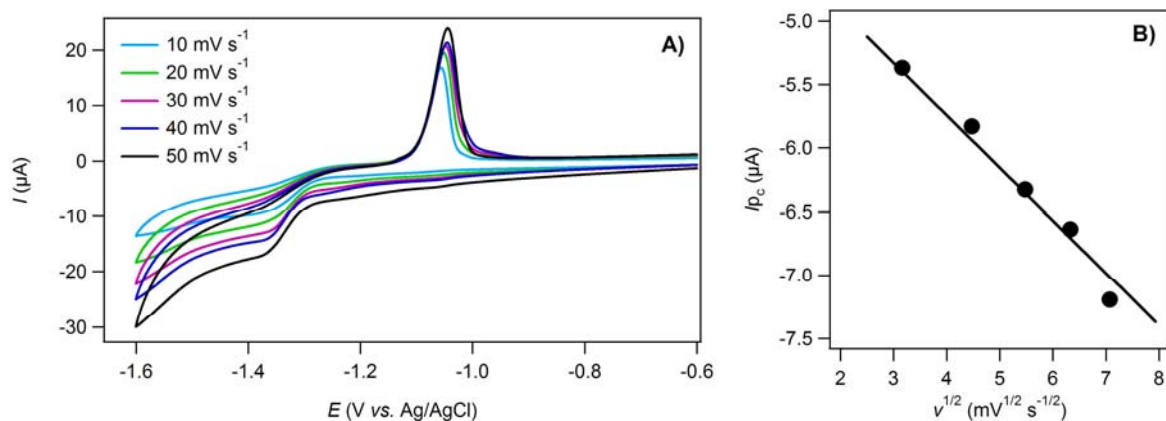


Fig. S4. (A) Cyclic voltammograms for ZnTPPC (1 mM) in a 0.1 M LiCl aqueous solution adjusted at pH 5.8 (working electrode: mercury film electrode) at different scan rates. (B) $I_{\text{pc}} = f(v^{1/2})$.

Photocurrent control experiments

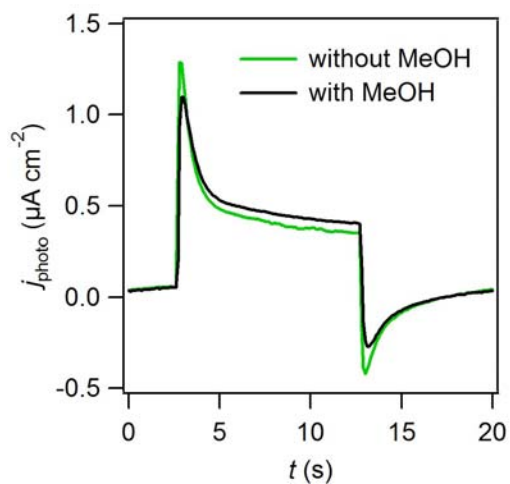


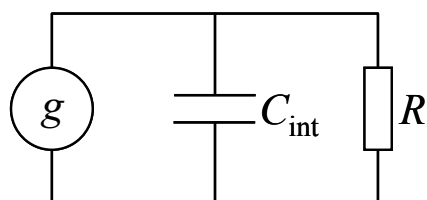
Fig. S5. Photocurrent transient measurement at 0.2 V obtained with the biphasic system containing 0.1 mM ZnTPPC (without gold NPs) and 1 mM Fc in the aqueous and DCE phases, respectively, with and without addition of methanol at the interface.

IMPS theory

The charge distribution across a liquid|liquid interface can be generally described by a simplified equivalent circuit consisting of a resistance R and an interfacial capacitance C_{int} in parallel (Scheme S1). This resistance R allows the relaxation of the flux of electrons injection g , which introduces an excess charge (depicted by C_{int}) at the interface and which can be expressed as:

$$g = ek_{\text{et}}\Gamma_{\text{S}}^* \quad (\text{S1})$$

where Γ_{S}^* corresponds to the surface density of the excited sensitizer (ZnTPPC* in our case) and e the elementary charge. This parameter g can be considered analogous to the flux of minority carriers determined by the Gärtner expression familiar from semiconductor photoelectrodes.^{1,2}



Scheme S1. Simplified equivalent circuit of the illuminated liquid|liquid interface.

The interfacial excess charge q_{int} can be calculated by resolution of the differential equation:

$$\frac{dq_{\text{int}}}{dt} = g - j_{\text{photo}} - ek_{\text{rec}}\Gamma_{[\text{S}\cdots\text{Q}^+]} \quad (\text{S2})$$

where j_{photo} stands for the photocurrent density and $\Gamma_{[\text{S}\cdots\text{Q}^+]}$ the surface density of the ions pair $[\text{S}\cdots\text{Q}^+]$ (where Q represents the quencher, *i.e.* Fc in our experiment).

From the equivalent circuit (Scheme S1), we can also write:

$$\frac{q_{\text{int}}}{C_{\text{int}}} = j_{\text{photo}}R \quad (\text{S3})$$

The resolution of the differential equation (S2) needs to know the surface densities Γ_{S}^* and $\Gamma_{[\text{S}\cdots\text{Q}^+]}$, which can be calculated from kinetic considerations.

Thus, the surface density Γ_{S}^* can be obtained from the differential equation:

$$\frac{d\Gamma_{\text{S}}^*}{dt} = I\sigma\Gamma_{\text{S}} - (k_{\text{et}} + k_{\text{d}})\Gamma_{\text{S}}^* \quad (\text{S4})$$

where Γ_{S} represents the surface density of the sensitizer in the ground state, σ the optical capture cross section and I the photon flux. In the presence of a periodic photon flux perturbation of angular frequency ω , the time-dependent incident illumination is of the form:

$$I = I_0 \exp(i\omega t) \quad (\text{S5})$$

Consequently, assuming quasi steady-state conditions, it follows that the surface density Γ_{S}^* is given by:

$$\Gamma_{\text{S}}^* = \frac{I\sigma\Gamma_{\text{S}}}{k_{\text{et}} + k_{\text{d}} + i\omega} \quad (\text{S6})$$

Similarly, the surface density $\Gamma_{[S^{\dots}Q^+]}$ can be determined from the differential equation:

$$\frac{d\Gamma_{[S^{\dots}Q^+]}}{dt} = k_{\text{et}}\Gamma_S^* - (k_{\text{rec}} + k_{\text{ps}})\Gamma_{[S^{\dots}Q^+]} \quad (\text{S7})$$

whose resolution leads to:

$$\Gamma_{[S^{\dots}Q^+]} = k_{\text{et}} \left(\frac{I\sigma\Gamma_S}{k_{\text{et}} + k_{\text{d}} + i\omega} \right) \left(\frac{1}{k_{\text{rec}} + k_{\text{ps}} + i\omega} \right) \quad (\text{S8})$$

Then, resolution of the differential equation (S2) can be performed, and it follows that the photocurrent density j_{photo} is given by:

$$j_{\text{photo}} = g \left(\frac{k_{\text{ps}} + i\omega}{k_{\text{rec}} + k_{\text{ps}} + i\omega} \right) \left(\frac{1}{1 + RC_{\text{int}}i\omega} \right) \quad (\text{S9})$$

where:

$$g = ek_{\text{et}} \left(\frac{I\sigma\Gamma_S}{k_{\text{et}} + k_{\text{d}} + i\omega} \right) \quad (\text{S10})$$

For low frequencies ($\omega \ll k_{\text{et}} + k_{\text{d}}$), g behaves like a scaling factor at a given potential and light intensity. Then the frequency dependent photocurrent normalized with respect to g can be expressed in terms of the real and imaginary components:

$$\frac{j_{\text{photo}}^{\text{re}}}{g} = \frac{k_{\text{ps}}(k_{\text{rec}} + k_{\text{ps}}) + \omega^2(1 + RC_{\text{int}}k_{\text{rec}})}{(1 + (RC_{\text{int}}\omega)^2)((k_{\text{rec}} + k_{\text{ps}})^2 + \omega^2)} \quad (\text{S11})$$

and:

$$\frac{j_{\text{photo}}^{\text{im}}}{g} = \frac{\omega(k_{\text{rec}} - RC_{\text{int}}(k_{\text{ps}}(k_{\text{rec}} + k_{\text{ps}}) + \omega^2))}{(1 + (RC_{\text{int}}\omega)^2)((k_{\text{rec}} + k_{\text{ps}})^2 + \omega^2)} \quad (\text{S12})$$

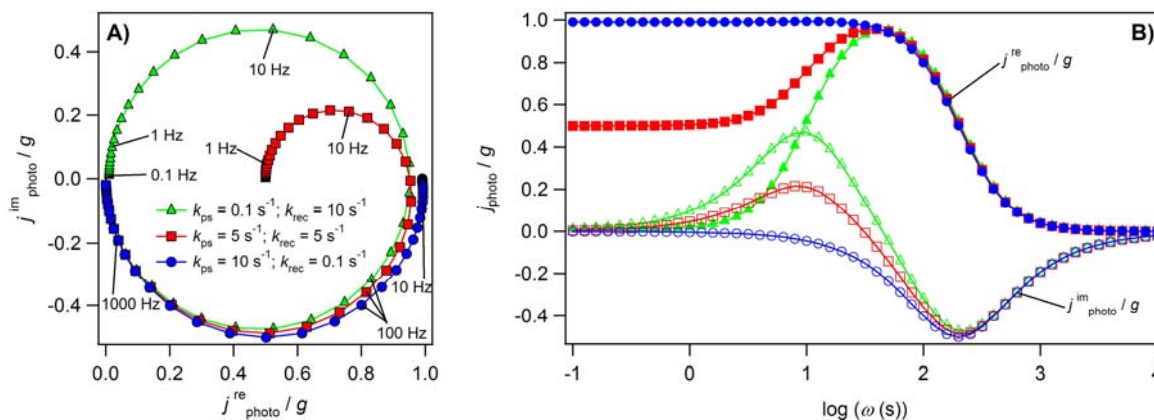


Fig. S6. (A) Complex representation and (B) “Bode” representation of simulated IMPS data calculated from eq. (17) and (18), taking $k_{\text{ps}} = 0.1 \text{ s}^{-1}$ and $k_{\text{rec}} = 10 \text{ s}^{-1}$ (\blacktriangle), $k_{\text{ps}} = k_{\text{rec}} = 5 \text{ s}^{-1}$ (\blacksquare) and $k_{\text{ps}} = 10 \text{ s}^{-1}$ and $k_{\text{rec}} = 0.1 \text{ s}^{-1}$ (\bullet), while the RC_{int} time constant was taken as 0.005 s^{-1} .

In Fig. S6B, the normalized real and imaginary components of the photocurrent response as a function of $\log(\omega)$ (“Bode” representation) are represented for three limiting cases, $k_{\text{ps}} \ll k_{\text{rec}}$, $k_{\text{ps}} = k_{\text{rec}}$ and $k_{\text{ps}} \gg k_{\text{rec}}$. For negligible recombination (Fig. S6B, circle-shaped symbols), the low frequencies limit of $j_{\text{photo}}^{\text{re}}/g$ approaches unity, while only negative values are obtained for

$j_{\text{photo}}^{\text{im}}/g$. For strong recombination (Fig. S6B, triangular-shaped symbols), the low frequencies limit of $j_{\text{photo}}^{\text{re}}/g$ tends to zero and $j_{\text{photo}}^{\text{im}}/g$ exhibits a positive maximum.

Representations of $j_{\text{photo}}^{\text{im}}/g$ vs. $j_{\text{photo}}^{\text{re}}/g$ (complex representation) for these different limiting cases are also displayed in Fig. S6A. The most interesting feature is that the IMPS data are extended into two quadrants of the complex plane since the phase shifts associated with the recombination effect and of the RC_{int} time constant effect have opposite signs. Thus, the low frequencies response is determined by the competition between k_{ps} and k_{rec} (semicircle in the upper quadrant), while the RC_{int} time constant dominates at higher frequencies (semicircle in the lower quadrant). Indeed, whatever the limiting case, the effect of the RC_{int} time constant becomes evident and the photocurrent is attenuated as the frequency is higher. If recombination becomes negligible (Fig. S6A, circle-shaped symbols), the lower the frequency is, the more exactly the photocurrent response follows the illumination (in-phase photocurrent response). As a result, the complex representation of the IMPS data is limited to the lower quadrant, and the normalized photocurrent occurs with an intercept at unity when the frequency tends toward zero. On the contrary, if recombination is not negligible (Fig. S6A, square and triangular-shaped symbols), this one becomes effective especially when the frequency is low ($\omega < k_{\text{rec}}$), and the comeback of the electrons through this recombination process leads to a semicircle in the upper quadrant. The bigger this semicircle is, the more important the ratio $k_{\text{rec}}/k_{\text{ps}}$ is. When the frequency increases ($\omega > k_{\text{rec}}$), the kinetic of the recombination process becomes too slow, and the phase difference decreases. Finally, the phase difference increases again at higher frequencies, the photocurrent response being attenuated by the RC_{int} time constant (leading to the semi-circle in the lower quadrant).

1. W. W. Gärtner, *Phys. Rev.*, 1959, **116**, 84-87.
2. L. M. Peter, *Chem. Rev.*, 1990, **90**, 753-769.